Applied Physics Letters

Photoelectrical reading in ZnO/Si NCs/*p*-Si resistive switching devices

Cite as: Appl. Phys. Lett. **116**, 193503 (2020); https://doi.org/10.1063/5.0005069
Submitted: 18 February 2020 . Accepted: 04 May 2020 . Published Online: 14 May 2020

J. López-Vidrier, J. L. Frieiro, O. Blázquez, D. Yazicioglu, S. Gutsch, K. E. González-Flores, M. Zacharias, S. Hernández, and B. Garrido

Applied Physics Letters ARTICLE scitation.org/journal/apl

Photoelectrical reading in ZnO/Si NCs/*p*-Si resistive switching devices

Cite as: Appl. Phys. Lett. **116**, 193503 (2020); doi: 10.1063/5.0005069
Submitted: 18 February 2020 · Accepted: 4 May 2020 ·
Published Online: 14 May 2020

J. López-Vidrier,[1,2,a)] J. L. Frieiro,[1,2] O. Blázquez,[3] D. Yazicioglu,[4] S. Gutsch,[4] K. E. González-Flores,[5] M. Zacharias,[4] S. Hernández,[1,2] and B. Garrido[1,2]

AFFILIATIONS

[1]MIND, Department of Electronic and Biomedical Engineering, Universitat de Barcelona, Martí i Franquès 1, E-08028 Barcelona, Spain
[2]Institute of Nanoscience and Nanotechnology (IN^{2}UB), Universitat de Barcelona, Av. Diagonal 645, E-08028 Barcelona, Spain
[3]Catalonia Institute for Energy Research (IREC), Jardins de les Dones de Negre 1, 2 pl., E-08930 Sant Adrià del Besòs (Barcelona), Spain
[4]Laboratory for Nanotechnology, IMTEK, Faculty of Engineering, University of Freiburg, Georges-Köhler-Allee 103, D-79110 Freiburg, Germany
[5]Centro de Investigación en Materiales Avanzados S.C. (CIMAV), Unidad Monterrey–PIIT, Apodaca, NL M-66628, Mexico

[a)]**Author to whom correspondence should be addressed:** jlopezv@ub.edu

ABSTRACT

The increasing need for efficient memories with integrated functionalities in a single device has led the electronics community to investigate and develop different materials for resistive switching (RS) applications. Among these materials, the well-known Si nanocrystals (NCs) have demonstrated to exhibit RS properties, which add to the wealth of phenomena that have been studied on this model material platform. In this work, we present ZnO/Si NCs/*p*-Si resistive switching devices whose resistance state can be electrically read at 0 V under the application of low-power monochromatic illumination. The presented effect is studied in terms of the inner structural processes and electronic physics of the device. In particular, the creation of conductive filaments through the Si NC multilayers induces a low-resistance path for photogenerated carriers to get extracted from the device, whereas in the pristine state charge extraction is strongly quenched due to the insulating nature of the NC-embedding SiO_2 matrix. In addition, spectral inspection of the generated photocurrent allowed unveiling the role of Si NCs in the reported effect. Overall, the hereby shown results pave the way to obtain memories whose RS state can be read under low-power conditions.

The resistive switching (RS) effect, which has been researched since the 1960s on resistive random-access memories (RRAMs) based on dielectric materials such as SiO_2,[1] has attracted great interest because of its potential application in non-volatile memory storage devices. The working principle of RS is the reduction of the dielectric resistance by several orders of magnitude (low resistance state, LRS), by enabling barrier-free (quasi-Ohmic) charge transport after adequate application of an external electric field (and consequent current) through the material. The main property of this effect is, however, its reversibility, since proper polarity can recover a high resistance state (HRS).[2] In some metal oxides, conductive filaments (CF) are created mainly obeying two mechanisms, namely the diffusion of metal atoms from the electrodes toward the dielectric (electrochemical metallization, ECM)[3] and the vacancy generation by oxygen ion diffusion from the dielectric toward the electrodes (valence change mechanism, VCM).[4] In addition, some groups have reported that light can also take part in RS, by either inducing stable CF formation (writing)[5,6] or reading the resistance state by means of electrical excitation (electroluminescence)[7,8] or optical transmittance (propagation losses in plasmonic waveguides),[9] in what is so far known as *optical memristor*. The study and development of these optical memristors can lead to a novel area of photonics-integrated memory devices.

The RS phenomenon has been widely studied in oxide materials, Si suboxides (SiO_x) being particularly interesting for the electronics industry because of their compatibility with complementary metal-oxide-semiconductor technology. Here, the works led by the group of Kenyon have highlighted the importance of electrode/dielectric interfaces in the CF formation process,[10,11] other studies being focused on

the adequacy of certain metals to the diffusion characteristics within Si-based matrices.[12] After a high-temperature annealing treatment, Si nanocrystals (NCs) can be produced, in which quantum confinement allows for improved and size-controlled electronic properties with respect to bulk Si.[13,14] Because of the wealth of optical and electrical phenomena that Si NCs exhibit, this material has served for many years as an adequate research platform for the study of semiconductors; nevertheless, only a few works exist on the RS properties of Si NCs.[8,15,16] In this regard, the electro-optical properties of Si NCs can be coupled to their RS to perform proof-of-concept optical memristors. In particular, we hereby propose a Si NC-based RS device where the resistance state can be read at 0 V by exhibiting a clear photocurrent response in LRS when exposed to low-power illumination.

To perform the present study, size-controlled Si NC multilayers (MLs) were prepared via the superlattice approach,[17,18] by depositing 5 × $SiO_{0.93}N_{0.23}$ [Si-rich Si oxynitride (SRON), 4.5 nm]/SiO_2(1 nm) bilayers on top of a (100) Si substrate (*p*-type, base resistivity of 1–20 Ω cm) using plasma-enhanced chemical vapor deposition (PECVD). Afterwards, a high-temperature annealing treatment was carried out at 1150 °C for 1 h in a N_2 ambient atmosphere, to induce phase separation, thus resulting in the precipitation of the Si excess (17 at. % at the selected stoichiometry) and its crystallization in the form of Si NCs. This process was followed by H_2 defect passivation at 450 °C for 1 h, to get rid of the undesired dangling bonds. Prior to the ML deposition, a 2-nm-thick Si_3N_4 interlayer was PECVD-deposited on top of the Si substrate, which improves the injection of minority carriers (electrons) from *p*-Si in substrate inversion conditions.[19] The device structure was achieved by depositing a 100-nm-thick ZnO layer on top of the MLs via atomic layer deposition (ALD) at 200 °C,[20,21] which acts as a transparent conductive electrode (almost negligible absorption throughout the visible range, conductivity $\sigma > 100\ \Omega^{-1}\,cm^{-1}$). A control sample was also fabricated containing neither the Si NC MLs nor the Si_3N_4 interlayer (i.e., ZnO ALD-deposited on top of the *p*-Si substrate). Conventional photolithography was then used to circularly pattern the ZnO electrodes (area $\sim 8 \times 10^{-3}\ cm^2$). Finally, the back contact was achieved by full-area Al deposition. The inset in Fig. 1(a) shows the schematic of the final device structure. Further details on material and device preparation can be found elsewhere.[22–25]

Electrical characterization [current–voltage $I(V)$ and current–time $I(t)$] of the devices was carried out at room temperature, in the dark and under illumination, using an Agilent B1500A semiconductor device analyzer connected to a probe station. The devices were polarized by applying voltage on the top ZnO electrode while grounding the Al-coated back contact. For measurements under monochromatic illumination, the devices were illuminated through the top ZnO electrode using either a 532-nm continuous wave laser (at power densities spanning from 0.1 to 200 mW cm^{-2}) or a Xe lamp coupled to a monochromator (reaching power densities of ∼0.5–2 mW cm^{-2} in the spectral range of 300–1100 nm). The spectral response (SR) was obtained by recording the current at each incident wavelength, once normalized by the corresponding optical power density.

To inspect the RS properties of the device structure, several devices were analyzed by means of $I(V)$ sweeping at both positive ($V > 0$, substrate inversion regime) and negative ($V < 0$, substrate accumulation regime) voltages. As shown in Fig. 1(a) for one representative device of the set, the employed device design exhibits bipolar RS behavior. To obtain these characteristics, a particular $I(V)$ protocol

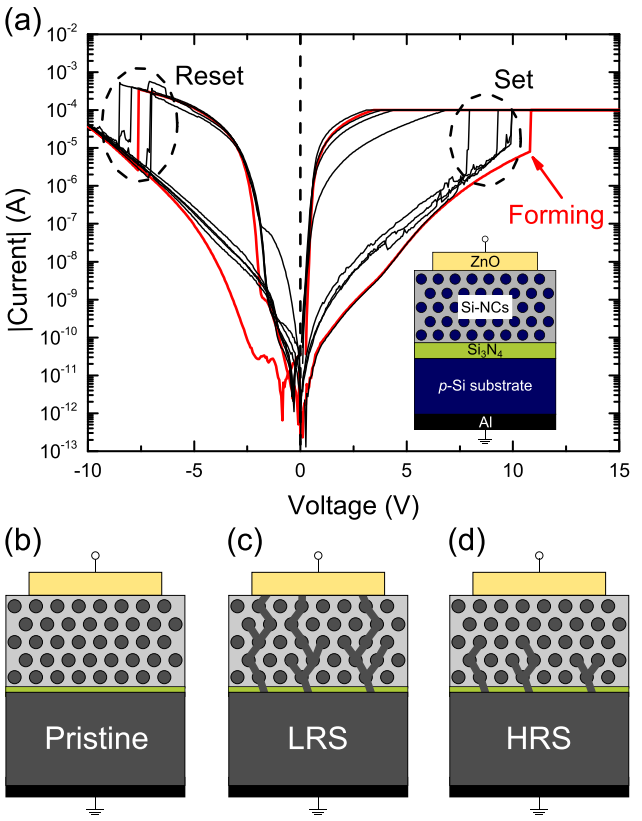

FIG. 1. (a) $I(V)$ characterization corresponding to the device under test. The *electroforming* cycle and four subsequent cycles are plotted in red and black, respectively. The *set* and *reset* processes are highlighted using dashed circles. The inset shows a sketch of the device structure. (b)–(d) Schematics showing the CF formation across the Si NC MLs: pristine (b), LRS (c), and HRS (d) states.

must be followed, whose steps are described in the following, the pristine state of the device [Fig. 1(b)] being the starting point. First, an increasing positive voltage is applied, which induces a gradual increase in current until a sudden change takes place around ∼11 V, after which the device exhibits higher conductivity, reaching the LRS. This initial process is called *electroforming*, and it has been previously attributed, in Si-rich oxide-related materials,[8,26] to the diffusion of loosely bound O^{2-} ions within the SiO_2 lattice toward the upper electrode (where a positive voltage has been applied); as a consequence, the generated O vacancies (V_O^{2+}) constitute at least one high-conductivity path, a CF, improving the electrical conduction of the Si NCs/SiO_2 multilayers [Fig. 1(c)]. In order to prevent excessive current to cause permanent damage to the device during this *electroforming* process, a current compliance of 100 μA was employed. Already under substrate accumulation ($V < 0$), the conductivity level is held high until reaching $V \sim -7.5$ V, where a sudden decrease occurs, obeying to a partial reoxidation of the generated CFs during the *electroforming* process, i.e., the *reset* process [Fig. 1(d)]. The device lies now within the HRS, where current levels resemble those corresponding to the pristine state of the device. After this first RS cycle [red color in Fig. 1(a)], subsequent $I(V)$ cycles exhibit similar processes, attaining the LRS (*set* process) at voltages between 8 V and 10 V, and HRS

(*reset*) at voltages between −6 V and −9 V; to attain lower *set* and *reset* voltages, a lower number of SRON/SiO_2 bilayers should be employed, as demonstrated in similar material systems in the literature.[15] Regarding the overall RS performance, our devices exhibit an evident conductivity variation between the LRS and the HRS, an I_{LRS}/I_{HRS} ratio of $\sim 10^4$–10^5 being measured at 3 V.

Please note that we have assumed the main CF generation taking place through the Si NCs. Indeed, this is the most plausible framework, since other works in the literature have demonstrated *in situ* creation of Si-rich regions in stoichiometric Si oxide after electric field application,[27] the group of Kenyon as well concluding that a CF is generated through Si-rich regions in SiO_x thin films.[26] In addition, the suboxide region surrounding the Si NC is likely to contain O vacancy-related defects,[28] which might enhance the local probability of CF generation. One last comment must be made regarding the ZnO electrode. In contrast to the clear RS effect observed in devices containing sputtered ZnO,[6,29] ALD-deposited ZnO was found to exhibit a high conductivity ($\sigma > 100\ \Omega^{-1}\,cm^{-1}$).[20,21] As a consequence, no RS takes place on the ZnO/*p*-Si reference device, even at applied voltages higher than 40 V, and therefore, no contribution of the electrode on the CF formation through the Si NC multilayers is expected.

So far, the device structure has demonstrated to behave as a bipolar RS device, exhibiting a clear difference between both resistance states in both voltage polarities. Taking profit of the easy-identifiable RS states, we inspected the impact of controlled illumination on the electrical properties at each state, using visible light. For this, we measured the evolution of current with time without applying any voltage, i.e., at $V = 0$ V, in the pristine, LRS, and HRS states from a single RS cycle in different devices. In Fig. 2(a), the $I(t)$ transients corresponding to each state from a representative device, both in the dark and under illumination (532-nm laser, ∼20 mW cm^{-2}), are plotted, where the change between dark and illumination is clearly indicated by vertical dashed lines. It is evident that the application of light induces an increase in current (photocurrent) in each resistance state, always well above the (dark) noise level (around $\sim 10^{-13}$ A, which is the resolution of our experimental setup). Actually, under illumination conditions, the change in current is much more pronounced for the LRS, reaching a current increase up to five orders of magnitude with respect to dark conditions. Instead, when operating in the pristine or in the HRS states, the current only increases up to one or two orders of magnitude, respectively, from the noise level. Several devices under test showed the same behavior. In addition, the RS state of the device was read during five cycles on the same device hereby presented, only showing a slight random dispersion in LRS and HRS photocurrent, and thus confirming that this observed difference between the LRS and HRS is not stochastic.

The measured current under illumination is coming from photocarrier generation promoted by the optical absorption of light either in the Si substrate or in the Si NCs (almost negligible absorption is expected in ZnO given its high transparency at the measured wavelength), whose extraction takes place thanks to the internal electric field created by the heterojunction (a negative flatband voltage around −2 V exists, according to capacitance–voltage measurements carried out in the past and reported in Ref. 19). This inner electric field is sufficiently intense to allow photogenerated electrons to sweep toward the top ZnO electrode and photogenerated holes to be collected by the Si substrate, which induces the extraction of a non-negligible current.

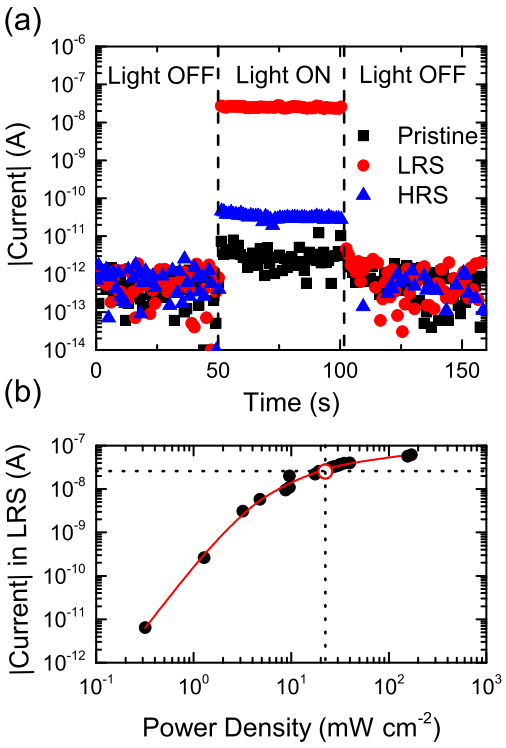

FIG. 2. (a) Time evolution of the current, at 0 V, corresponding to the device under study (from Fig. 1) under 532-nm laser excitation, for each RS state: pristine (black squares), LRS (red circles), and HRS (blue triangles). Vertical dashed lines indicate the time when light was switched on and off. (b) Laser power density dependence of the average current level of the device while in the LRS. The laser power conditions employed in (a) correspond to the red open circle. Black full circles represent the experimental data, whereas the red line serves as a guide to the eye.

Although this occurrence can take place in any of the resistance states under study, the SiO_2 barriers state a main drawback for the extraction of photogenerated carriers when the device lies in the pristine and HRS states (as confirmed by the low current levels reached under illumination). In contrast, the CFs present in the LRS notably enhance carrier extraction of the system, thus resulting in a clearly different electrical response between LRS and HRS under illumination, around ∼3 orders of magnitude. Finally, to push the device to its detection limit, we measured the generated photocurrent in the LRS under different laser power densities, whose results are plotted in Fig. 2(b). We could observe a sizeable signal even at values as low as ∼0.3 mW cm^{-2}, which corresponds to a power of 2.4×10^{-6} W after considering the device area (totally illuminated in our experiment). This optical power is about two orders of magnitude lower than the required one for reading the LRS only by electrical means [the power in LRS at a read value of 3 V is about $\sim 1.8 \times 10^{-4}$ W, see Fig. 1(a)]. Furthermore, we could also extrapolate our measurements to pulsed excitation for evaluating the energy consumption of the reading process. Assuming that capacitive effects are not relevant in the LRS (at least in the ns-regime), and considering excitation pulses of a duration of 10 ns (in agreement with current works in RS devices),[30] the energy employed for the lowest-power consumption photoelectrical reading of the LRS would be 2.4×10^{-14} J, well below the pJ limit exhibited by other RS

systems in the literature employing only electrical means.[30] Overall, our results show that our RS system state can be photoelectrically read, which supposes a lower power consumption than if purely electrical means were to be considered.

To elucidate the photogeneration origin within the device structure, we proceeded with the spectral analysis of the electrical response of the LRS, at 0 V and using monochromatic excitation from 300 to 1100 nm [power density of ~0.5–2 mW cm^{-2}, above the device sensitivity limit, as shown in Fig. 2(b)]. The obtained SR, once adequately normalized to the energy of the incident photons, yields the external quantum efficiency [EQE = SR × $(h \times c)/(q \times \lambda)$, h being Planck's constant, c the speed of light in vacuum, q the elementary charge, and λ the associated wavelength to the incident photon], which represents, at each incoming wavelength, the number of extracted photocarriers per incident photon. Figure 3 plots the EQE spectrum (at 0 V) corresponding to the device under study in the LRS (red circles), and that from a control device only containing the p-Si substrate with ALD-deposited ZnO on top (black squares), which exhibits a direct electrical connection between these two materials. Given the low power density of the monochromatic source, no EQE spectrum could be obtained from the device under test, at 0 V, either in the pristine or HRS states; instead, the spectrum corresponding to the pristine state was acquired at 8 V for the sake of comparison (blue triangles). It is important to note that the EQE spectrum from the device under test still presents a sizeable EQE in the transparency region of Si NCs ($\lambda > 1000$ nm),[31] arising from carrier photogeneration in the bulk Si substrate. When comparing the EQE of the device in the LRS to the Si NC-free reference device, three pieces of evidence immediately arise: the NC-based device in LRS exhibits (i) a much lower EQE (about three orders of magnitude), (ii) a change in the EQE line shape, and (iii) a blueshift of the EQE low-energy edge.

On the one hand, the limited photocurrent extracted from the devices containing Si NCs—observation (i)—could be ascribed to the presence of insulating layers (SiO_2 and Si_3N_4), which notably hinder

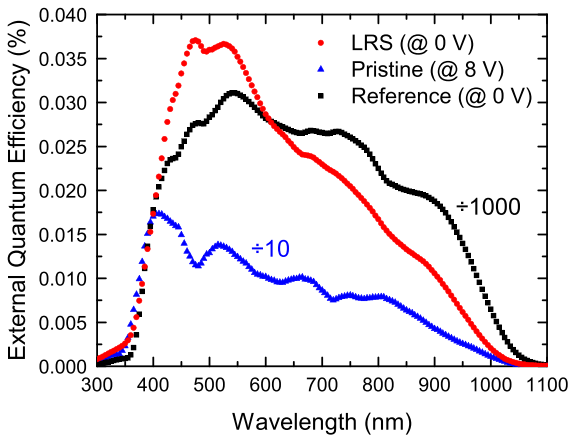

FIG. 3. External quantum efficiency spectra, obtained under illumination and at 0 V, corresponding to the device under study while in the LRS state (red circles), and acquired at 8 V while in the pristine state (blue triangles). The EQE corresponding to a ZnO/p-Si reference device, at 0 V, is provided as Si NC-free reference (black squares). The pristine state and reference EQE spectra are respectively divided by a factor 10 and 1000 to match with the signal level of the test device in the LRS.

the photogenerated carrier extraction; moreover, in the case of the LRS, the defective nature of the CF (or CFs)[32] might reduce the carrier diffusion length. Actually, the generated V_O^{2+} that constitutes the CF may generate a local region with mixing of those compounds (Si, SiO_x, and/or SiN_x) that, together with its defective nature and its limited cross section, could be contributing to limit the overall carrier extraction. On the other hand, observations (ii) and (iii) suggest that the Si NC/SiO_2 MLs contribute to carrier photogeneration in the LRS. The EQE line shape for the device containing the NCs—observation (ii)—presents a more pronounced feature at shorter wavelengths, which is compatible with the larger density of states in this range of energies for nanostructured Si.[33,34] Finally, the fact that there is a blueshift of the EQE edge at longer wavelengths—observation (iii)—also indicates a higher bandgap energy than bulk Si, compatible with carrier quantum confinement within Si NCs.[13,14] Indeed, the EQE spectrum at 8 V corresponding to the pristine state of the same NC-containing device confirms both observations (low-energy edge blueshift and more efficient high-energy photoresponse). Therefore, the three pieces of evidence are in agreement with Si NCs playing an important role in the electrical properties under illumination after *electroforming*, where the carriers are preferentially extracted through the CFs, i.e., the lower-resistance paths.

In summary, the clear influence of the Si NCs to the EQE of the device under study in the LRS must necessarily be linked to the CFs. Bearing in mind that carriers are mainly absorbed by either the Si NC MLs or the Si substrate (CFs present a much lower cross section compared to the device area), they need to be collected by the CFs and sent to the external circuit. Photogenerated carriers at the Si substrate can easily be driven by the built-in electric field toward the electrodes through the CF. Instead, only carriers photogenerated at NCs close to the CFs will be able to be extracted and thus contribute to photocurrent, since the NC MLs do not present a percolated network at the employed Si excess.[35,36] Due to the fact that the size of the exciton in Si is around 5–10 nm, the presence of an unique CF would result in a poor carrier extraction from Si NCs. Thus, and given that evidence through direct observation is still lacking in the research area, it is plausible to believe that a dense network of CFs should be created across the whole ML stack, giving rise to an effective medium that is electrically connected in the vertical direction.

The hereby presented results have shown that the ZnO/Si NC MLs/p-Si structure not only exhibits RS properties, but also that its resistance states can be unequivocally distinguished at 0 V by its exposure to low-power light. Here, the role of Si NC MLs is important, since (i) the presence of SiO_2 ensures a bottleneck for photocarrier extraction under the HRS (and it therefore limits, or even prevents, photocurrent signal) and (ii) tuning the NC size might help selecting the light wavelength to which the LRS resistance state could be read. Overall, we have demonstrated a RS device structure whose memory state can be read under ambient light using zero electrical power, which paves the way to a future integration of Si NC-based RS devices into photonic integrated circuits.

This work was financially supported by the German Research Foundation (Nos. ZA191/27-3 and ZA191/33-1) and the Spanish Ministry of Economy, Industry and Competitiveness (No. TEC2016-76849-C2-1-R). J.L.-V. and J.L.F., respectively, acknowledge financial support from a "*Juan de la Cierva*"

postdoctoral fellowship (No. IJCI-2017-33451) from the Spanish Ministry of Economy, Industry and Competitiveness, and the subprogram "*Ayudas para la Formación de Profesorado Universitario*" (No. FPU16/06257) from the Spanish Ministry of Education, Culture and Sports.

DATA AVAILABILITY

The data that support the findings of this study are available from the corresponding author upon reasonable request.

REFERENCES

[1]D. R. Lamb and P. C. Rundle, J. Appl. Phys. **18**, 29 (1967).
[2]I. Valov, ChemElectroChem **1**, 26 (2014).
[3]I. Valov, R. Waser, J. R. Jameson, and M. N. Kozicki, Nanotechnology **22**, 289502 (2011).
[4]R. Waser, R. Dittmann, G. Staikov, and K. Szot, Adv. Mater. **21**, 2632 (2009).
[5]A. Mehonic, T. Gerard, and A. J. Kenyon, Appl. Phys. Lett. **111**, 233502 (2017).
[6]O. Blázquez, J. L. Frieiro, J. López-Vidrier, C. Guillaume, X. Portier, C. Labbé, S. Hernández, and B. Garrido, Appl. Phys. Lett. **115**, 261104 (2019).
[7]W. Lin, K. Zhu, Y. Su, H. Shi, Y. Meng, and H. Zhao, Appl. Phys. Lett. **112**, 133504 (2018).
[8]J. L. Frieiro, J. López-Vidrier, O. Blázquez, D. Yazıcıoğlu, S. Gutsch, J. Valenta, S. Hernández, M. Zacharias, and B. Garrido, J. Appl. Phys. **126**, 144501 (2019).
[9]C. Hoessbacher, Y. Fedoryshyn, A. Emboras, A. Melikyan, M. Kohl, D. Hillerkuss, C. Hafner, and J. Leuthold, Optica **1**, 198 (2014).
[10]A. Mehonic, M. S. Munde, W. H. Ng, M. Buckwell, L. Montesi, M. Bosman, A. L. Shluger, and A. J. Kenyon, Microelectron. Eng. **178**, 98 (2017).
[11]M. S. Munde, A. Mehonic, W. H. Ng, M. Buckwell, L. Montesi, M. Bosman, A. L. Shluger, and A. J. Kenyon, Sci. Rep. **7**, 9274 (2017).
[12]S. Sonde, B. Chakrabarti, Y. Liu, K. Sasikumar, J. Lin, L. Stan, R. Divan, L. E. Ocola, D. Rosenmann, P. Choudhury, K. Ni, S. K. R. S. Sankaranarayanan, S. Dattad, and S. Guha, Nanoscale **10**, 9441 (2018).
[13]F. Iacona, G. Franzò, and C. Spinella, J. Appl. Phys. **87**, 1295 (2000).
[14]F. Iacona, G. Franzò, V. Vinciguerra, A. Irrera, and F. Priolo, Opt. Mater. **17**, 51 (2001).
[15]K. E. González–Flores, B. Palacios-Márquez, J. Álvarez–Quintana, S. A. Pérez–García, L. Licea-Jiménez, P. Horley, and A. Morales-Sánchez, Nanotechnology **29**, 395203 (2018).
[16]K. E. González-Flores, P. Horley, S. A. Cabañas-Tay, S. A. Pérez-García, L. Licea-Jiménez, L. Palacios-Huerta, M. Aveces-Mijares, M. Moreno-Moreno, and A. Morales-Sánchez, Superlattices Microstruct. **137**, 106347 (2020).
[17]M. Zacharias, J. Heitmann, R. Scholz, U. Kahler, M. Schmidt, and J. Bläsing, Appl. Phys. Lett. **80**, 661 (2002).
[18]J. López-Vidrier, S. Hernández, D. Hiller, S. Gutsch, L. López-Conesa, S. Estradé, F. Peiró, M. Zacharias, and B. Garrido, J. Appl. Phys. **116**, 133505 (2014).
[19]J. López-Vidrier, S. Gutsch, O. Blázquez, J. Valenta, D. Hiller, J. Laube, J. Blanco-Portals, L. López-Conesa, S. Estradé, F. Peiró, B. Garrido, S. Hernández, and M. Zacharias, Adv. Electron. Mater. **4**, 1700666 (2018).
[20]J. Laube, D. Nübling, H. Beh, S. Gutsch, D. Hiller, and M. Zacharias, Thin Solid Films **603**, 377 (2016).
[21]H. Beh, D. Hiller, J. Laube, S. Gutsch, and M. Zacharias, J. Vac. Sci. Technol., A **35**, 01B127 (2017).
[22]A. M. Hartel, D. Hiller, S. Gutsch, P. Löper, S. Estradé, F. Peiró, B. Garrido, and M. Zacharias, Thin Solid Films **520**, 121 (2011).
[23]S. Gutsch, J. Laube, A. M. Hartel, D. Hiller, N. Zakharov, P. Werner, and M. Zacharias, J. Appl. Phys. **113**, 133703 (2013).
[24]J. López-Vidrier, Y. Berencén, S. Hernández, O. Blázquez, S. Gutsch, J. Laube, D. Hiller, P. Löper, M. Schnabel, S. Janz, M. Zacharias, and B. Garrido, J. Appl. Phys. **114**, 163701 (2013).
[25]J. López-Vidrier, S. Gutsch, O. Blázquez, D. Hiller, J. Laube, R. Kaur, S. Hernández, B. Garrido, and M. Zacharias, Appl. Phys. Lett. **110**, 203104 (2017).
[26]A. Mehonic, S. Cueff, M. Wojdak, S. Hudziak, O. Jambois, C. Labbé, B. Garrido, R. Rizk, and A. J. Kenyon, J. Appl. Phys. **111**, 074507 (2012).
[27]J. Yao, L. Zhong, D. Natelson, and J. M. Tour, Sci. Rep. **2**, 242 (2012).
[28]A. Zimina, S. Eisebitt, W. Eberhardt, J. Heitmann, and M. Zacharias, Appl. Phys. Lett. **88**, 163103 (2006).
[29]O. Blázquez, J. L. Frieiro, J. López-Vidrier, C. Guillaume, X. Portier, C. Labbé, P. Sanchis, S. Hernández, and B. Garrido, Appl. Phys. Lett. **113**, 183502 (2018).
[30]M. Lanza, H.-S. P. Wong, E. Pop, D. Ielmini, D. Strukov, B. C. Regan, L. Larcher, M. A. Villena, J. J. Yang, L. Goux *et al.*, Adv. Electron. Mater. **5**, 1800143 (2019).
[31]S. Mirabella, R. Agosta, G. Franzò, I. Crupi, M. Miritello, R. Lo Savio, M. A. Di Stefano, S. Di Marco, F. Simone, and A. Terrasi, J. Appl. Phys. **106**, 103505 (2009).
[32]J. Robertson and R. Gillen, Microelectron. Eng. **109**, 208 (2013).
[33]G. Ledoux, O. Guillois, D. Porterat, C. Reynaud, F. Huisken, B. Kohn, and V. Paillard, Phys. Rev. B **62**, 15942 (2000).
[34]D. Kovalev, H. Heckler, D. Polisski, J. Diener, and F. Koch, Opt. Mater. **17**, 35 (2001).
[35]S. Gutsch, D. Hiller, J. Laube, M. Zacharias, and C. Kübel, Beilstein J. Nanotechnol. **6**, 964 (2015).
[36]J. Laube, S. Gutsch, D. Wang, C. Kübel, M. Zacharias, and D. Hiller, Appl. Phys. Lett. **108**, 043106 (2016).